Disease-specific imaging with H-scan trajectories and support vector machine to visualize the progression of liver diseases

Jihye Baek
Department of Electrical and Computer Engineering
University of Rochester
Rochester, NY, USA
jbaek7@ur.rochester.edu

Kevin J. Parker
Department of Electrical and Computer Engineering
University of Rochester
Rochester, NY, USA
kevin.parker@rochester.edu

Abstract— **To uniquely identify diseases utilizing the H-scan analysis, we proposed a new imaging method called disease-specific imaging (DSI). As a supervised learning method, it requires training with medical images and corresponding tag labels. In this study, we trained our DSI using ultrasound liver images and their pathological confirmation, including fibrosis, steatosis, and pancreatic ductal adenocarcinoma (PDAC) metastasis. From the ultrasound data, we extracted three features of H-scan % blue, attenuation coefficient, and B-scan intensity. These were assigned as inputs for the DSI training. First, support vector machine (SVM) training constructed decision planes to identify liver conditions. Second, disease axes were defined by calculating a linear fit line from each disease cluster. The trained DSI can discriminate between distinct liver conditions and visualize the severity of each disease using color images overlaid on B-scan images.**

The SVM training achieved 100% classification accuracy and is capable of differentiating normal, early, and late stages of each disease. The scans were obtained from three different animal models and ultrasound scanners, but our uniform approach efficiently unified the multiparametric analysis. The H-scan trajectories and DSI can be useful to both diagnose and track the progression of liver disease.

Keywords—H-scan ultrasound, Tissue classification, Support vector machine, Disease-specific imaging

I. Introduction

The scope of quantitative ultrasound measurements has increased, enabling better assessment of pathological tissue changes. Specifically, the H-scan analysis has derived parameters which can contribute to tissue classifications of inflammation, fibrosis, steatosis, and tumor in liver [1-4]. In addition to classification, tracking the steady progression of diseases or their response to therapy requires more accurate measurements. The H-scan analysis has also demonstrated trajectories of multiparametric features over time [5].

By utilizing quantitative measurements extracted from medical images, the support vector machine (SVM) is one of the widely used machine learning methods for classification [6-8]. Since SVM training uses data points near class boundaries, which are support vectors, it can have an advantage when collecting a large number of data sets is challenging, as in the field of medical imaging [9, 10]. Moreover, the lack of data, which may cause overfitted results, can be compensated for by optimizing the parameters of SVM to obtain smooth and robust hyperplanes [4]. However, the classification results, including hyperplanes, are only shown in parameter space separated from the original medical images. To understand the meaning of hyperplanes with multiple parameters, background knowledge about the parameters is required. Also, SVM classification does not provide degrees of closeness to the hyperplanes, which can be related to diseases progression.

To address the limitations, we proposed disease-specific imaging (DSI) which incorporates the SVM and inner-product. The DSI approach can classify liver diseases and show a simple visual display of disease progression. The proposed method was applied to *in vivo* studies. This framework is capable of monitoring the progression of different liver diseases including steatosis, fibrosis, and tumor metastasis.

II. Materials and Methods

A. Feature extraction

We extracted three features from the ultrasound signals: H-scan percent blue (% blue), attenuation coefficient, and B-scan intensity.

a) H-scan analysis: The H-scan is a matched filter analysis to characterize scattering signatures from tissues, resulting in color-coded images [11]. Our H-scan approach is extended to estimate spectral shifts of reflected echoes at high spatial resolution, and the frequency estimates were mapped into color levels varying from 1 to 256, which corresponds to colors gradually changing from red to blue [12]. Thus, the color can represent relative sizes of scatterers, where more red and blue colors indicate relatively larger and smaller scatterers, respectively. The color display is quantified by % blue: (number of blue pixels)/(total number of pixels)×100% where the pixels with color levels of 1-128 and 129-256 are red and blue pixels, respectively. The % blue parameter was normalized by setting % blue = 50% for normal livers.

b) Attenuation estimation: Ultrasound propagation through media causes attenuation along the depth direction, which leads to a frequency downshift over depth. The H-scan approach is capable of measuring the downshift, enabling estimation of the attenuation coefficient α (dB/MHz/cm) [4].

c) B-scan: B-scan intensity was calculated in log-compressed scale (I_{dB}). Since B-scan intensity measurement varies depending on the ultrasound scanner

2021 IEEE International Ultrasonics Symposium (IUS) | 978-1-6654-0355-9/21/$31.00 ©2021 IEEE | DOI: 10.1109/IUS52206.2021.9593627

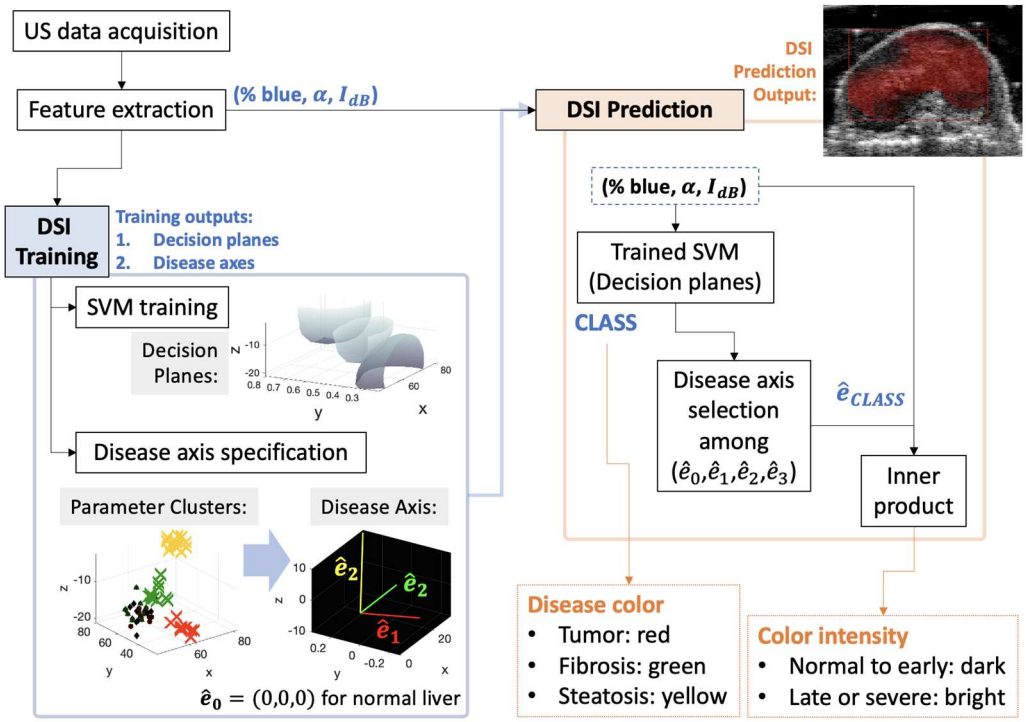

Fig. 1. DSI flow chart.

used, this parameter was also normalized by setting intensity at -15 dB for normal livers.

B. *Disease-specific imaging*

DSI procedures are summarized in **Fig. 1**. DSI requires training, and the trained DSI predicts liver conditions. Training consists of two main steps: (1) SVM training which constructs decision planes to identify liver diseases, and (2) disease axis specification, where multiparametric analysis defines disease axes by calculating each cluster's linear fit line. Once the DSI is trained, it can predict disease conditions for any new ultrasound scans. For the prediction, DSI first extracts features from the ultrasound signal: (% blue, α, I_{dB}). The trained SVM classifies liver states, resulting in CLASS; in this study, the states can be tumor, fibrosis, steatosis, or normal liver. According to the CLASS, one disease axis is selected among the four disease axes, where the disease axes have unit vectors ($\hat{e}_0$,$\hat{e}_1$,$\hat{e}_2$,$\hat{e}_3$). Then, the unit vector of the selected axis can be written by $\hat{e}_{CLASS}$. Lastly, the inner product between the measured features and the unit vector of the selected disease axis is calculated: $\hat{e}_{CLASS} \cdot$ (% blue, α, I_{dB}). The inner product result becomes the color intensity of each pixel. Normal to early stages have lower intensity, whereas late or severe stages have higher intensity; the colors corresponding to the intensities are provided with color bars in **Fig. 3**. Based on CLASS, DSI selects a color, and we set red, green, and yellow colors for tumor, fibrosis, and steatosis. For the pixels classified as normal tissues, the inner product results in 0 since the unit vector is $\hat{e}_0 = (0,0,0)$, and therefore the pixels show only B-scan gray scale intensity without color overlay.

C. *Animal study*

In vivo mouse studies were performed independently to induce (1) pancreatic ductal adenocarcinoma (PDAC) metastasis by injecting pancreatic tumor cells (KCKO-luc) [13], (2) fibrosis by exposure to carbon tetrachloride [4], and (3) steatosis by feeding a methionine and choline deficient diet [1]. 32 animals were enrolled: 9 C57BL/6J mice for PDAC study; 7 Sprague-Dawley and 4 TAC NIHRNU for fibrosis; 12 Sprague-Dawley for steatosis. Disease progression was monitored once or twice per week using ultrasound. Final disease stages were confirmed with pathology.

D. *Ultrasound data acquisition*

To acquire ultrasound data from the three disease models of PDAC metastasis, fibrosis, and steatosis, we used three ultrasound scanners; Vantage 256 (Verasonics, Inc.,

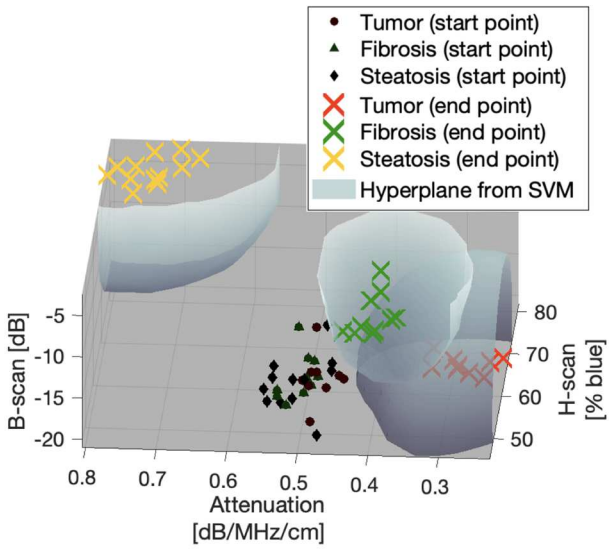

Fig. 2. SVM training resulted in 100% accuracy.

Kirkland, WA, USA) equipped with an L11-5v transducer (10 MHz center frequency) for the tumor model; Vevo 2100 (FUJIFILM VisualSonics, Toronto, ON, Canada) with a MS 250 linear probe (21 MHz center frequency) for fibrosis; and Vevo 3100 (FUJIFILM VisualSonics, Toronto, ON, Canada) utilizing a MX 201 linear probe (15 MHz center frequency) for steatosis. The Verasonics system transmitted plane wave with 25 angles from -6 to 6 degrees, generating IQ data. The VisualSonics machines transmitted focused beam and provided RF data.

Ultrasound scans were performed once or twice per week to monitor disease progression, and a total of 2778 frames were acquired for DSI training.

III. Results and Discussion

The three features (% blue, α, I_{dB}) were measured, which formed clusters in multiparametric space as shown in **Fig. 2**. Early time points before inducing the diseases formed a cluster of normal liver. Late time points, that were confirmed as severe stages of diseases by histology, resulted in the three clusters of steatosis, fibrosis, and PDAC metastasis. These four groups were input tags for SVM training. The training achieved 100% classification accuracy and constructed hyperplanes as shown in **Fig. 2**.

For DSI, the features were classified by SVM, and feature changes over time were quantified with each disease axis using the inner product. The classification resulted in the colors of yellow, green, and red for steatosis, fibrosis, and tumor, respectively, as shown in **Fig. 3**. The quantification determines color levels, inferring the severity of each disease. The color levels are visualized using the provided color bars, where the darker color on the left side and the brighter color on the right side represent normal/early and severe/late stages, respectively. Since the first column shows images of normal or early-stage disease, there is no overlaid color. From left to right, the diseases progressed; therefore the color overlaid area increased, and the overlaid colors became more vivid.

We investigated the color images obtained by the trained DSI and demonstrated that the color images changed as the diseases progressed, thus DSI can monitor the disease progression of fibrosis, steatosis, and PDAC metastasis. However, quantitative evaluation of the imaging results remains for further investigation. For example, disease segmentation by DSI may be compared with other gold standard measurements, such as diseased area defined in histology slides. This will permit an assessment of the accuracy of DSI over a range of different pathologies.

IV. Conclusion

We proposed the DSI approach based on H-scan trajectories, which enables a visualization of both diagnosis and disease progression. This approach differentiated normal, early, and late stages of fibrosis, steatosis, and PDAC metastasis. The three diseases were investigated with three different animal models and ultrasound scanners, but our uniform approach efficiently unified the multiparametric analysis. Furthermore, we anticipate clinical use of the DSI utilizing ultrasound images or other imaging modalities that can extract multiple parameters.

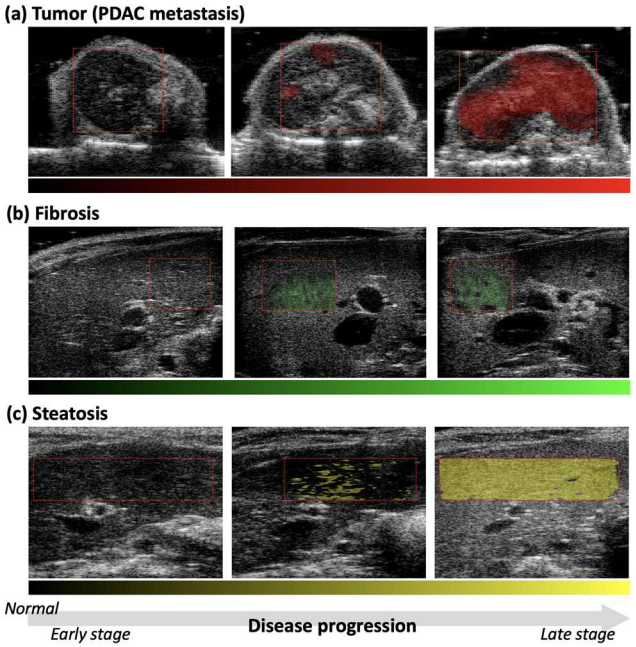

Fig. 3. DSI results. (a) PDAC metastasis. (b) Fibrosis. (c) Steatosis. The colors of red, green, and yellow represent classified pixels of tumor, fibrosis, and steatosis, respectively. The color bars indicate disease progressive levels; early to severe stages shows dark to bright colors. From left to right columns, the diseases progressed, and therefore the colors became more vivid over time. The left column showing normal stages does not have overlaid color. The second column have more color overlaid area, and in the images of the third column showing severe stage, most of the pixels within the red region-of-interest boxes shows overlaid colors.

Acknowledgment

This work was supported by National Institutes of Health grant R21EB025290. The authors are grateful to colleagues who conducted three different studies and who scanned liver models and provided RF data, including Rifat Ahmed and Marvin Doyley at the University of Rochester, Terri Swanson and Theresa Tuthill at Pfizer Inc., and Kenneth Hoyt and Lokesh Basavarajappa at the University of Texas at Dallas.

References

[1] J. Baek, S. S. Poul, L. Basavarajappa *et al.*, "Clusters of Ultrasound Scattering Parameters for the Classification of Steatotic and Normal Livers," *Ultrasound in Medicine & Biology*, 2021.

[2] L. Basavarajappa, J. Baek, S. Reddy *et al.*, "Multiparametric ultrasound imaging for the assessment of normal versus steatotic livers," *Scientific Reports,* vol. 11, no. 1, Jan 29, 2021.

[3] J. Baek, T. A. Swanson, T. Tuthill *et al.*, "Support vector machine (SVM) based liver classification: fibrosis, steatosis, and inflammation," *Proceedings of the 2020 Ieee International Ultrasonics Symposium (Ius)*, 2020.

[4] J. Baek, S. S. Poul, T. A. Swanson *et al.*, "Scattering Signatures of Normal Versus Abnormal Livers with Support Vector Machine Classification," *Ultrasound in Medicine and Biology,* vol. 46, no. 12, pp. 3379-3392, Dec, 2020.

[5] J. Baek, and K. J. Parker, "H-scan trajectories indicate the progression of specific diseases," *Medical Physics*, Aug 3, 2021.

[6] J. Virmani, V. Kumar, N. Kalra *et al.*, "SVM-Based Characterization of Liver Ultrasound Images Using Wavelet

Packet Texture Descriptors," *Journal of Digital Imaging,* vol. 26, no. 3, pp. 530-543, Jun, 2013.

[7] W. J. Wu, S. W. Lin, and W. K. Moon, "Combining support vector machine with genetic algorithm to classify ultrasound breast tumor images," *Comput Med Imaging Graph,* vol. 36, no. 8, pp. 627-33, Dec, 2012.

[8] C.-Y. Chang, S.-J. Chen, and M.-F. Tsai, "Application of support-vector-machine-based method for feature selection and classification of thyroid nodules in ultrasound images," *Pattern recognition,* vol. 43, no. 10, pp. 3494-3506, 2010.

[9] V. N. Vapnik, "An overview of statistical learning theory," *Ieee Transactions on Neural Networks,* vol. 10, no. 5, pp. 988-999, Sep, 1999.

[10] C. Cortes, and V. Vapnik, "Support-vector networks," *Machine learning,* vol. 20, no. 3, pp. 273-297, 1995.

[11] K. Parker, "The H-scan format for classification of ultrasound scattering," *OMICS J. Radiol,* vol. 5, no. 5, pp. 1000236, 2016.

[12] K. J. Parker, and J. Baek, "Fine-tuning the H-scan for discriminating changes in tissue scatterers," *Biomedical Physics & Engineering Express,* vol. 6, no. 4, Jul, 2020.

[13] J. Baek, R. Ahmed, J. Ye *et al.*, "H-Scan, Shear Wave and Bioluminescent Assessment of the Progression of Pancreatic Cancer Metastases in the Liver," *Ultrasound in Medicine and Biology,* vol. 46, no. 12, pp. 3369-3378, Dec, 2020.